CONCRETE LIBRARY OF JSCE NO. 14, MARCH 1990

HYSTERETIC BEHAVIOR OF A PARTIALLY BONDED PRESTRESSED CONCRETE RIGID FRAME UNDER LATERAL LOADING

(Translation from Proceedings of JSCE, No.396/V-9, Aug. 1989)

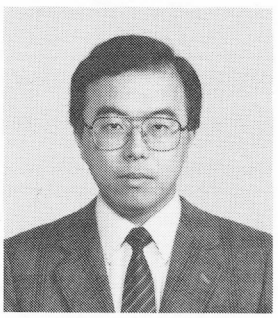

Hidetaka UMEHARA

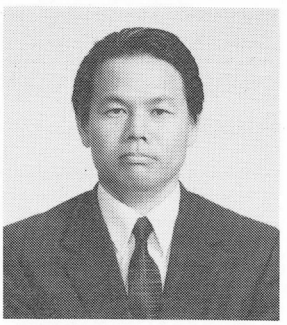

Tada-aki TANABE

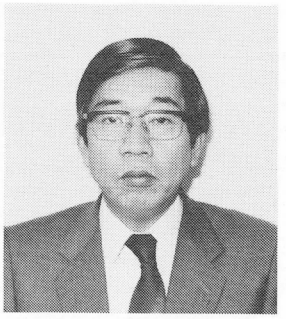

Hirotomo YOSHIDA

SYNOPSIS

The finite element analysis is developed in order to estimate the hysteretic behavior of prestressed concrete structures in partially bonded condition under cyclic loading considering non-linear stress-strain relation of concrete and steel. The method is applied to the bonded and unbonded prestressed concrete beams and rigid framed structures composed of precast concrete members and connected by prestressing steel, and the deformations and the angle of rotation observed in the experiment are compared with the calculated values. The mathematical model to express the rotation at jointed corner and the effects of initial prestress and bonded condition to the hysteretic behavior under cyclic loading are discussed.

Hidetaka UMEHARA is an associate professor of Civil Engineering at Nagoya Institute of Technology, Nagoya, JAPAN. He received his Doctor of Philosophy in 1982 from the University of Texas at Austin. His research interests include thermal effects on concrete structures and behaviors of reinforced concrete structures under seismic loading. He is a member of JSCE, JCI, and ACI.

Tada-aki TANABE is a professor of Civil Engineering at Nagoya University, Nagoya, JAPAN. He received his Doctor of Engineering in 1971 from the University of Tokyo. He is the chairman of JCI Committee on the Thermal Stress of Massive Concrete Structures besides a member of various committees of JSCE, JCI, and ACI. His main research is directed to the dynamic failure mechanism of RC structures besides the thermal stress.

Hirotomo YOSHIDA is a professor of Civil Engineering and Dean of Student Bureau at Nagoya Institute of Technology, Nagoya, JAPAN. He received his Doctor of Engineering in 1963 from the University of Tokyo. He is the chairman of JCI Committee on Educational Activities besides a member of various committees of JSCE, JCI, and ACI. His main research activities are in the area of chemical admixtures for concrete, uses of slag and special cement, and massive concrete.

---

1. INTRODUCTION

Recently, unbonded prestressed concrete structures have been built increasingly with the development of prestressing steel which has improved resistance to corrosion thus reducing the grouting work and shortening the process of construction. Furthermore, the use of precast members connected by unbonded tendons to form a rigid frame has been tried increasingly.

The monotonic and hysteretic behavior of prestressed concrete structures of this type is far different from the one with concrete and prestressing steel in bonded condition. In addition to it, the prestressed concrete member is usually considered to be in the fully bonded condition, when cement milk is grouted in sheaths. However, it is often in partially bonded condition and its behavior is between the ones with bonded and unbonded condition. If this is the case, it may be said that their dynamic characteristics are not yet fully clarified and their theoretical investigations are rather scarce.

The analysis of the prestressed concrete members partially bonded was made by the authors for elastic condition [1]. In this study, the method is developed to include more general cases with material non-linearity.

The method is applied to estimate the hysteretic behavior of prestressed concrete beams and a rigid framed structure under cyclic loading and the results are compared with the experimental results to verify its accuracy.

In the case of the rigid framed structures composed of precast concrete members connected by prestressing steel, the rotation at jointed corner affects the behavior under cyclic loading. Hence, the modeling of jointed corner is tried as well to make clear these behavior.

2. THEORETICAL CONSIDERATION

2.1 Modeling of The Stress Strain Relations for Concrete and Tendon under Cyclic Loading

The stress strain relations for concrete and tendon under cyclic loading as shown in Fig. 1 are used for the analysis of the prestressed concrete members partially bonded. The stress-strain curve for tendon is assumed to be bilinear. The stress-strain curve for concrete is assumed to be quadratic before the strain reaches $2000X10^{-6}$ and the stress decreases as strain increases from $2000X10^{-6}$ to $10000X10^{-6}$. For reversed loading, when the maximum experienced compressive strain is less than $300X10^{-6}$ corresponding to the stress about $f_c'/3$, unloading path is assumed to be linear to zero stress. When it is from $300X10^{-6}$ to $2000X10^{-6}$, unloading path follows the line which connect the maximum experienced strain point and the point which coordinate is (1+1/6) of the maximum experienced strain and a half of the maximum experienced stress, and after that decreases linearly to the residual strain which is equal to 1/6 of the maximum experienced strain. When it is more than $2000X10^{-6}$, unloading path is exactly same as the line which unloading path of the maximum experienced strain equal to $2000X10^{-6}$ follows, except that the maximum experienced strain is different and the unloading point is different. Tensile strength of concrete is ignored. When the signs change from tension to compression under reversal loading, the compressive stress occurs after the strain exceeds the maximum residual strain in each subdivided element, and increases linearly to the point which has the maximum experienced strain. The tangential modulus is taken for the tangential slope of the stress-strain curve at the strain occurring in the subdivided element under cyclic loading.

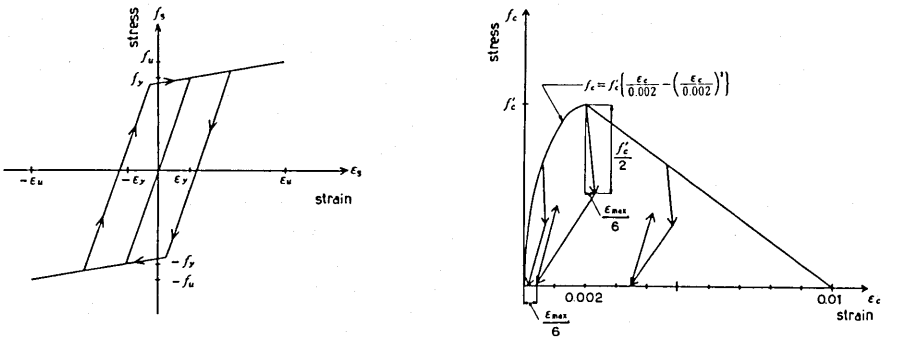

(a) prestressing steel (b) concrete

Fig. 1 Stress-strain curves

2.2 Strain Energy Equation of A Beam Element in A Prestressed Concrete Member under Partially Bonded Condition

Two more basic assumptions in addition to the stress strain relation mentioned before are made when deriving a strain energy equation of a beam element in a prestressed concrete member under partially bonded condition.
(a) Plane concrete sections before bending remain plane after bending.
(b) A shear deformation is zero.

The incremental potential energy equation in partially bonded condition of concrete and prestressing steel is expressed as

$$\Delta\pi=\Delta U_c+\Delta U_s+\Delta V+\Delta U_f \tag{1}$$

Each term of Eq.(1) is derived from the following equations.

(1) ΔU_c is written as the summation of an increment of strain energy at each loading step as shown in the following equation of concrete in a system which comprises of several members. When a tendon exists in a member, the member is defined as a beam portion which length is exactly same as a tendon length.

$$\Delta U_c=\sum_{i=1}^{ELM}\frac{1}{2}\int_{VOL}E_c(p)\,\Delta\varepsilon_{ci}^2\,dV \tag{2}$$

where, ELM : number of element within a system
$E_c(p)$: tangential modulus of concrete at each loading increment
p : stress path

(2) ΔU_s is defined as an increment of strain energy of tendons, and varies according to the extent of bondage of concrete and tendon. If the condition is perfectly bonded and there is no sliding between concrete and tendon, the strain increment of tendon should be equal to the strain increment of concrete at the same place. However, in the unbonded condition, a strain increment of tendon $\Delta\varepsilon_{sa}$ of any place of a member is same as shown in Fig. 2. Hence, $\Delta\varepsilon_{sa}$ is given as

$$\Delta\varepsilon_{sa}=\frac{1}{L}\int_0^L\Delta\varepsilon_{cs}\,dx \tag{3}$$

where, L denotes length of tendon

In general cases, the bonded condition may exist between two described cases and a strain increment of tendon $\Delta\varepsilon_s$ is written in the following equation.

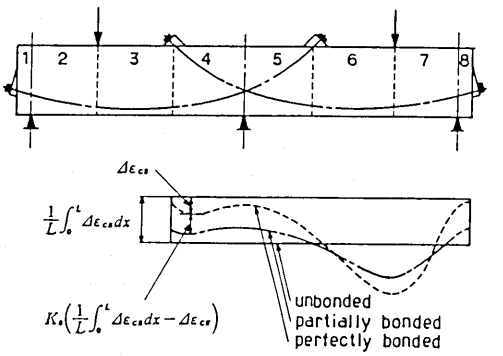

Fig. 2 Steel strain distribution affected by the bond condition

$$\Delta\varepsilon_s = K_s\left(\frac{1}{L}\int_0^L \Delta\varepsilon_{cs}dx - \Delta\varepsilon_{cs}\right) + \Delta\varepsilon_{cs} \tag{4}$$

where, K_s is defined as the sliding coefficient and constant value of K_s from 0 to 1 indicates the extent of bondage of a partially bonded prestressed concrete member. When $K_s=0$, Eq.(4) corresponds to the fully bonded condition and when $K_s=1$, Eq.(4) corresponds to the unbonded condition.

Using Eq.(4), ΔU_s is rewritten as follows,

$$\Delta U_s = \sum_{k=1}^{MEM}\sum_{j=1}^{NCA}\frac{1}{2}\int_0^{L_{jk}} E_s(p)\,A_{sjk}\left[K_s\left(\frac{1}{L_{jk}}\int_0^{L_{jk}}\Delta\varepsilon_{cs}dx - \Delta\varepsilon_{cs}\right) + \Delta\varepsilon_{cs}\right]^2 dx \tag{5}$$

where, MEM : number of members within a system
NCA : number of tendons within a member
$E_s(p)$: Young's modulus of tendon at each loading increment
p : stress path
A_{sjk} : area of j tendon in k member
L_{jk} : length of j tendon in k member

(3) ΔV is defined as increment of external energy due to each loading increment.

$$\Delta V = -\sum_{i=1}^{JNT}[\Delta P_i(u_{2i}-u_{1i}) + \Delta F_i(v_{2i}-v_{1i}) + \Delta M_i(\theta_{2i}-\theta_{1i})] - \sum_{i=1}^{ELM}\int_0^{l_i}\Delta q_i(v_{2i}-v_{1i})\,dx \tag{6}$$

where, JNT : number of joints
ΔP_i : increment of axial load at i node
ΔF_i : increment of load perpendicular to the member axis at i node
ΔM_i : increment of moment at i node
q_i : increment of distributed load at i element
u_{ji} : increment of deflection along x axis at i node in j loading step
v_{ji} : increment of deflection along y axis at i node in j loading step
θ_{ji} : increment of rotation at i node in j loading step

(4) ΔU_f is defined as an increment of energy dissipated by sliding friction between concrete and tendon. The displacements of concrete and tendon at x from the edge of a member are given as $\int_0^x \Delta\varepsilon_{cs}dx$ and $\int_0^x \Delta\varepsilon_s dx$.

The relative displacement caused by sliding friction is written as

$$\Delta x=\int_0^x(\Delta\varepsilon_s-\Delta\varepsilon_{cs})\,dx$$
$$=\int_0^x\left[K_s\left(\frac{1}{L}\int_0^L\Delta\varepsilon_{cs}dx-\Delta\varepsilon_{cs}\right)\right]dx \tag{7}$$

When $F_r(x)$ is defined as a friction force working at x, ΔU_f is expressed as

$$\Delta U_f=\sum_{k=1}^{MEMNCA}\sum_{j=1}^{}\int_0^{L_{jk}}\Delta x_{jk}F_r(x)\,dx \tag{8}$$

It is possible to assume $F_r(x)=\alpha\Delta x$ and deal with ΔU_f in the same way as ΔU_s. However, α depends on the type of structure and the shape of tendon, etc. As the behavior of prestressed concrete structures after prestressing is mainly discussed in this study, ΔU_f principally concerned with the prestressing may be ignored.

2.2 DERIVATION OF STIFFNESS MATRIX

Displacement increments are expressed using displacement function $[N_u]$ and $[N_v]$ as

$$\Delta u^e=[N_u]\{\Delta d_u^e\}$$
$$\Delta v^e=[N_v]\{\Delta d_v^e\} \tag{9}$$

where, Δu^e and Δv^e are displacement increments in a beam element and Δd_u^e and Δd_v^e are displacement increments at a node along x and y axis, respectively, as shown in Fig.3.

Strain increment along x axis in a beam element is written as,

$$\Delta\varepsilon_x^e=\Delta u^{e\prime}-y\Delta v^{e\prime\prime}$$
$$=[N_u',\ -yN_v'']\begin{Bmatrix}\Delta d_u^e\\ \Delta d_v^e\end{Bmatrix} \tag{10}$$

Substituting Eq.(10) into Eq.(2) yields,

$$\Delta U_c=\sum_{i=1}^{ELM}\frac{1}{2}\int_{VOL}E_c(p)(\Delta u^{e\prime}-y\Delta v^{e\prime\prime})^2dV$$
$$=\sum_{i=1}^{ELM}\frac{1}{2}\int_{VOL}E_c(p)\Delta d_i^TT_i^TG_i^TG_iT_i\Delta d_i\,dV \tag{11}$$

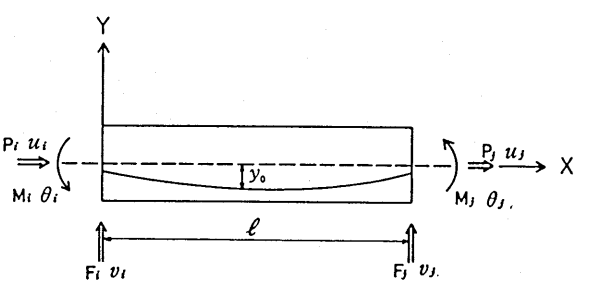

Fig. 3 Sign convention for a beam element

where, $G_i=[N'_u, -yN''_v]$

T_i : transformation matrix

$$\Delta d_i^e=\begin{Bmatrix}\Delta d_u^e\\ \Delta d_v^e\end{Bmatrix},\quad \Delta d_i=\begin{Bmatrix}\Delta d_u\\ \Delta d_v\end{Bmatrix},\quad \Delta d_i^e=T_i\Delta d_i$$

Substituting Eq.(10) into Eq.(5) yields,

$$\Delta U_s=\sum_{k=1}^{MEMNCA}\sum_{j=1}\frac{(1-K_s)^2}{2}A_{sjk}\sum_{i=1}^{ELM}\int_0^{l_{ijk}}E_s(p)(\Delta u^{e\prime}-y_{0ijk}\Delta v^{e\prime\prime})^2\,dx$$

$$+\sum_{k=1}^{MEMNCA}\sum_{j=1}\frac{K_s^2}{2L_{jk}^2}A_{sjk}\left(\sum_{i=1}^{ELM}\int_0^{l_{ijk}}E_s(p)\,dx\right)\left[\sum_{i=1}^{ELM}\int_0^{l_{ijk}}(\Delta u^{e\prime}-y_{0ijk}\Delta v^{e\prime\prime})\,dx\right]^2$$

$$+\sum_{k=1}^{MEMNCA}\sum_{j=1}\frac{K_s(1-K_s)}{L_{jk}}A_{sjk}\left[\sum_{i=1}^{ELM}\int_0^{l_{ijk}}E_s(p)(\Delta u^{e\prime}-y_{0ijk}\Delta v^{e\prime\prime})\,dx\right]\left[\sum_{i=1}^{ELM}\int_0^{l_{ijk}}(\Delta u^{e\prime}-y_{0ijk}\Delta v^{e\prime\prime})\,dx\right]$$

$$=\sum_{k=1}^{MEMNCA}\sum_{j=1}\frac{(1-K_s)^2}{2}A_{sjk}\sum_{i=1}^{ELM}\int_0^{l_{ijk}}E_s(p)\,\Delta d_i^TT_i^TH_i^TH_iT_i\Delta d_i dx+\sum_{k=1}^{MEMNCA}\sum_{j=1}\frac{K_s^2}{2L_{jk}^2}A_{sjk}\left(\sum_{i=1}^{ELM}\int_0^{l_{ijk}}E_s(p)\,dx\right)$$

$$\Delta d_i^TS_j^TS_j\Delta d_i+\sum_{k=1}^{MEMNCA}\sum_{j=1}\frac{K_s(1-K_s)}{L_{jk}}A_{sjk}\left(\sum_{i=1}^{ELM}\int_0^{l_{ijk}}E_s(p)\,\Delta d_i^TT_i^TH_i^Tdx\right)S_j\Delta d_i \qquad (12)$$

where, $H_i=[N'_u, y_{0ijk}N''_v]$

$$S_j=\sum_{i=1}^{ELM}\int_0^{l_{ijk}}H_iT_i\,dx$$

y_{oijk} : distance from neutral axis to jth tendon at i element in k member

The increment of external energy corresponding to Eq.(6) is rewritten as,

$$\Delta V=-\sum_{i=1}^{JNT}\Delta F_iT_i\Delta d_i-\sum_{i=1}^{ELM}\int_0^{l_i}\Delta q_iN_iT_i\Delta d_i\,dx$$

$$=-\sum_{i=1}^{JNT}\Delta d_i^TT_i^T\Delta F_i^T-\sum_{i=1}^{ELM}\int_0^{l_i}\Delta q_i\Delta d_i^TT_i^TN_i^T\,dx \qquad (13)$$

where, ΔF_i : vector of force increment at i node

$$\Delta F_i=\begin{Bmatrix}\Delta P_i\\ \Delta F_i\\ \Delta M_i\end{Bmatrix}$$

Δq_i : vector of distributed load increment at i element

$N_i=[N_u, N_v]$

Using minimum potential energy theory, Eq.(1) is rewritten as,

$$\frac{\partial\Delta\pi}{\partial\Delta d_i}=\frac{\partial\Delta U_c}{\partial\Delta d_i}+\frac{\partial\Delta U_s}{\partial\Delta d_i}+\frac{\partial\Delta V}{\partial\Delta d_i}$$

$$=\sum_{i=1}^{ELM}\int_{VOL}E_c(p)\,T_i^TG_i^TG_iT_i\Delta d_i dV+\sum_{k=1}^{MEMNCA}\sum_{j=1}(1-K_s)^2A_{sjk}\sum_{i=1}^{ELM}\int_0^{l_{ijk}}E_s(p)\,T_i^TH_i^TH_iT_i\Delta d_i\,dx$$

$$+\sum_{k=1}^{MEMNCA}\sum_{j=1}\frac{K_s^2}{L_{jk}^2}A_{sjk}\left(\sum_{i=1}^{ELM}\int_0^{l_{ijk}}E_s(p)\,dx\right)S_j^TS_j\Delta d_i+\sum_{k=1}^{MEMNCA}\sum_{j=1}\frac{2K_s(1-K_s)}{L_{jk}}A_{sjk}\left(\sum_{i=1}^{ELM}\int_0^{l_{ijk}}E_s(p)\right.$$

$$T_i^T H_i^T dx\Big) S_j \Delta d_i - \sum_{i=1}^{JNT} T_i^T \Delta F_i^T - \sum_{i=1}^{ELM} \int_0^{l_i} \Delta q_i T_i^T N_i^T dx = 0 \tag{14}$$

Therefore, finally stiffness matrix is expressed as,

$$\{[K_c]+[K_{s1}]+[K_{s2}]\}\{\Delta d_i\}=[F] \tag{15}$$

where,

$$[K_c]=\sum_{i=1}^{ELM}\int_{VOL} E_c(p)\, T_i^T G_i^T G_i T_i dV \tag{16-a}$$

$$[K_{s1}]=\sum_{k=1}^{MEMNCA}\sum_{j=1}^{} (1-K_s)^2 A_{sjk} \sum_{i=1}^{ELM} \int_0^{l_{ijk}} E_s(p)\; T_i^T H_i^T H_i T_i dx \tag{16-b}$$

$$[K_{s2}]=\sum_{k=1}^{MEMNCA}\sum_{j=1}^{} \frac{K_s^2}{L_{jk}^2} A_{sjk} \Big(\sum_{i=1}^{ELM}\int_0^{l_{ijk}} E_s(p)\, dx\Big) S_j^T S_j$$

$$+\sum_{k=1}^{MEMNCA}\sum_{j=1}^{} \frac{2K_s(1-K_s)}{L_{jk}} A_{sjk} \Big(\sum_{i=1}^{ELM}\int_0^{l_{ijk}} E_s(p)\; T_i^T H_i^T dx\Big) S_j \tag{16-c}$$

$$[F]=\sum_{j=1}^{JNT} T_i^T \Delta F_i^T + \sum_{i=1}^{ELM} \int_0^{l_i} \Delta q_i T_i^T N_i^T dx \tag{16-d}$$

When the tensile strain exceeds the limit of cracking strain at any place in a element, the crack opens at that place. As the stress intensity varies within a element, tangential modulus also varies within a element. Hence, each element is subdivided into M times N subelements in x direction and in y direction respectively as shown in Fig. 4, and the stress-strain relationship is applied at each subdivided element. Therefore, Eq.(16-a) is rewritten as the summation of stiffness of each subdivided element.

$$[K_c]=\sum_{i=1}^{ELM} b \sum_{k=1}^{N}\sum_{j=1}^{M} E_c(i,j,k,p)\, T_i^T G_i^T G_i T_i \tag{17}$$

For example, stiffness of one element $[K_{c11}]$ is expressed as, for the case that T_i is a unit matrix,

$$K_{c11}=\sum_{i=1}^{ELM}\int_{VOL} \frac{b}{l_i^2} E_c(p)\, dV$$

$$=\sum_{i=1}^{ELM} \frac{1}{l_i^2} \sum_{k=1}^{N}\sum_{j=1}^{M} (q_{k+1}-q_k)\, b_k (r_{j+1}-r_j)\, E_c(i,j,k,p) \tag{18}$$

where, b_k : width of element

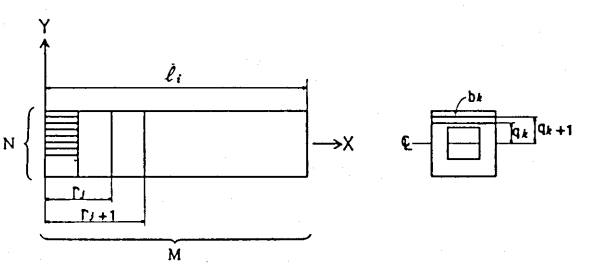

Fig. 4 A subdivided element

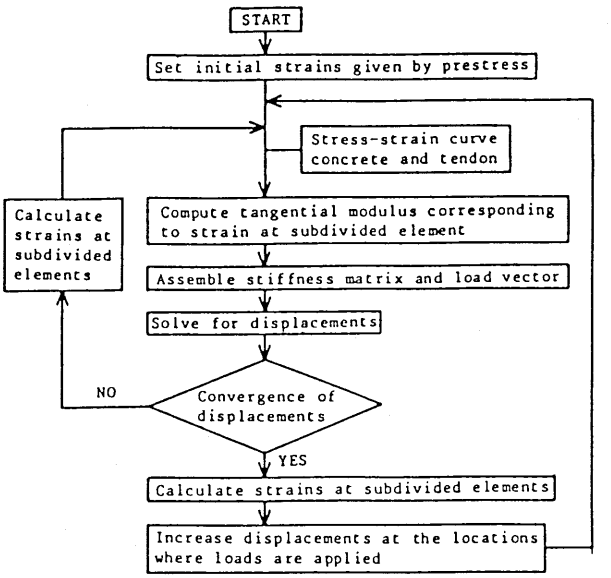

Fig. 5 Flow chart for iterative processes

Prestress effect is considered treating ε_{CP} shown in the following equation in a beam element as initial strain.

$$\varepsilon_{CP}=\frac{P}{E_c(p)}\left(\frac{1}{A_c}+\frac{y_o}{I_c}y\right) \tag{19}$$

where, A_c : area of cross section
y_o : distance from neutral axis to tendon
I_c : moment of inertia
P : load of tendon after prestressing

The analysis is carried out following the flow chart shown in Fig. 5. When a displacement is forced at a node at i step, the stiffness matrix is constructed first using tangential modulus at i-1 step, and the unknown displacement increments at other nodes are calculated by Eq.(15). Strain increment at each subdivided elements are calculated from the displacement increments, and tangential modulus at the strain is obtained from the stress-strain relationship shown in Fig. 1. Hence, the stiffness matrix is revised and the displacement increment at each node is obtained again. Iteration is conducted until displacement increment at i step becomes constant. In calculation, the total error of displacement increment is less than 5 % and the equivalent nodal force $[\Delta F]_n$ caused by the error is added to the load at i+1 step as shown in the following equation.

$$\{[K_c]_{n+1}+[K_{s1}]_{n+1}+[K_{s2}]_{n+1}\}\{\Delta \boldsymbol{d}\}_{n+1}=[\boldsymbol{F}]_{n+1}+[\Delta \boldsymbol{F}]_n \tag{20}$$

3. COMPARISON OF THE ANALYSIS WITH TEST RESULTS OF PRESTRESSED CONCRETE BEAMS

The proposed method of analysis is applied to the test results of prestressed concrete beams subjected to cyclic loading conducted by Okada et al [2]. The experiment aims to compare the behavior of an unbonded beam to that of a bonded beam when more than 90 % load of maximum capacity of a beam is applied

cyclically. The specimens are simple beams with 100 cm length as shown in Fig. 6 and cyclic load is applied at two symmetrical points of the span. The cross section of the test specimen has a 10 cm width and 15 cm depth, and 2 tendons with 7.4 mm diameter (yield point=141 kg/mm^2, tensile strength=150 kg/mm^2) are used. Compressive strength of concrete is 443 kg/cm^2 and initial prestress is 58 kg/cm^2.

Figures 7 and 8 indicate the comparison of the experimental and the analytical hysteresis loops of load-deflection curve in the case of bonded and unbonded prestressed beam, respectively. In the analysis, displacement is controlled at each loading step to obtain the hysteresis loop following the flow chart in Fig. 5. From the figures, it is evident that the unbonded beam shows the more pronounced reversed S shape curve and larger deflection than that in bonded beam in the experiments. The unbonded beam indicates as well that the ability of energy absorption represented by the area surrounded by the loop is less. As for the analytical load-deflection curves, the analytical results in both cases of bonded(K_s=0.0) and unbonded(K_s=1.0) beams indicate almost similar tendency to experimental ones, although the area surrounded by the loop in the analysis are a little less than that in the experiment. In the analysis it is also evident that the hysteresis loop in the unbonded beam has more pronounced reversed S shape than that in the bonded beam. Furthermore, the analysis indicates that under first cycle of loading the maximum stress of concrete reaches about 90% of the strength and tendons do not exceed yield point, and under second cycle, the maximum stress of concrete reaches the strength and in the case of bonded beam tendons exceed yield point, which are indeed the observed behavior by the experiment. From these comparisons, the analytical method is said to be able to follow the behavior of prestressed concrete beams under cyclic loading with reasonable accuracy.

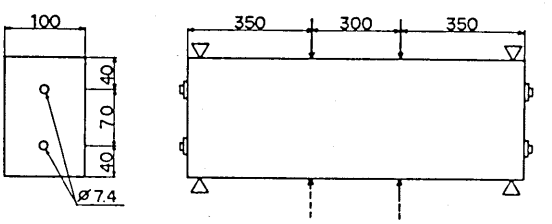

Fig. 6 The beam specimen and the loading scheme

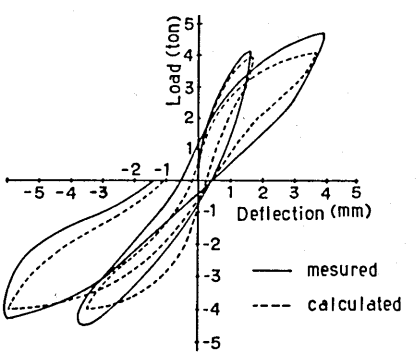

Fig. 7 Load-deflection curves in the bonded beam

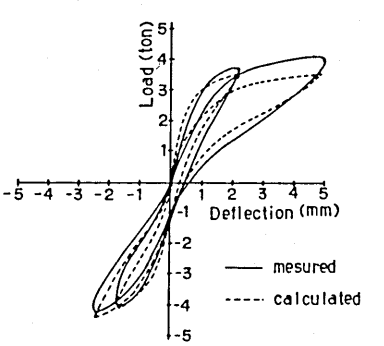

Fig. 8 Load-deflection curves in the unbonded beam

3. THE HYSTERETIC BEHAVIOR OF A PRECAST PRESTRESSED RIGID FRAME

One of the characteristics in the behavior of a rigid framed structure composed of precast concrete members connected by prestressing steels is that rotation of the jointed corner is largely affected by the condition of bond and the amount of prestress. This behavior is indicated for an important problem in the seismic responce analysis of a composite framed structure [3]. Therefore, the appropriate modeling of the jointed corner is developed to realize the behavior.

π shaped specimens composed of a beam and two columns connected by two prestressing bars with 22 mm diameter were tested as shown in Fig. 9 [3]. The cross section of the beam is 20x40 cm and the length is 180 cm and the cross section of the column is 20x30 cm and its length is 130 cm. Three specimens tested are ungrouted and grouted ones with 50 kg/cm^2 initial prestress, and grouted one with 35 kg/cm^2 initial prestress. The specimens are set on two roller supports and subjected to lateral load which is applied at the place 90 cm far from the jointed corner in the column.

The rotation at the corner was measured using contact gages and wire strain gages on concrete and tendons. Figure 10 shows the relationship between applied moment and measured rotation. It indicates that at the same applied moment the measured rotation at the corner in ungrouted specimen is almost twice as large as that in grouted specimen. While, the rotation at failure in the specimen with 35 kg/cm^2 initial prestress is almost half of that in the specimen with 50 kg/cm^2 initial prestress.

The developed method was applied to the structural system of this experiment assuming a special corner element shown by the shaded area in Fig. 11. The assumption of the special corner element is closely related to the assumption that a plane section remains plane after bending, which is used in a beam

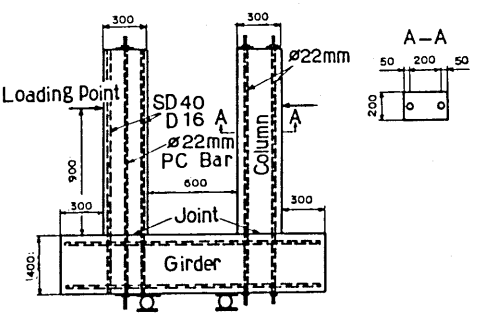

Fig. 9 The π shaped specimen

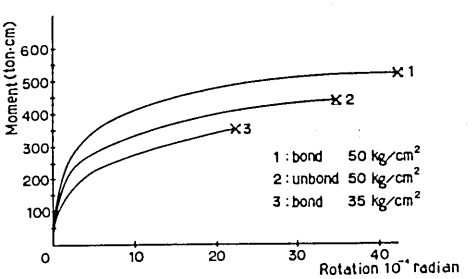

Fig. 10 Measured rotations at three different types of specimens

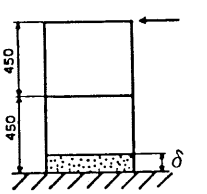

Fig. 11 The model for calculating rotation at a jointed corner

element. At the corner, this plane section assumption is not appropriate as large strain concentration in compressive zone will violate the assumption. The area with softer rigidity and limited width where the assumption do not consist may be expressed as a special element. Roughly, the rate of contribution to rotation of this portion may be expressed as some constant values of the rotation E/δ from Eq.(21) using similarlity to a spring constant.

$$\frac{1}{S} = \frac{\theta}{M} = \frac{1}{M}\int_0^{\delta} \frac{M}{EI} dx \fallingdotseq \frac{1}{M} \cdot \frac{M\delta}{EI} = \frac{\delta}{EI} \qquad (21)$$

where, S : spring constant
θ : rotation
I : average moment of inertia of the area
δ : the width of the area

Hence, the appropriate values for δ and E are investigated. Figure 12 shows the relationship between calculated rotation and applied moment in the unbonded specimen. When concrete stiffness is used at the corner element, the result shows that while the maximum moment is almost the same as that in tested specimen, the rotation at the jointed corner is much less than measured one. It means that the corner element with smaller stiffness is needed. The analytical results using the elements with δ=2 cm, E=50000 kg/cm^2, δ=4 cm, E=100000 kg/cm^2, and δ=6 cm, E=150000 kg/cm^2 indicate the similar behavior to that of tested specimens. In these three cases, E/δ is equal to 25000 kg/cm^3. In other words, the area which do not follow the plane section assumption may be simulated by the spring of which spring constant is 25000xI kg·cm.

Figures 13 and 14 show the analytical results in the bonded specimens with 50 kg/cm^2 and 35 kg/cm^2 initial prestress using three models, respectively. In both cases, the analytical results indicate that similar values to the experimental data are obtained. It should be noted here that when sliding coefficient K_s is equal to 0.7, best agreement is obtained. It means that at the tested specimens, grouted motar filled in the sheath was not strong enough to assure the full bondage. It is also considered that the diameter of tendon is 22 mm and bond failure in the specimen with this tendon occurs more easily than in that with smaller tendon such as 7.4 mm, because in the case of the grouted beam with 7.4 mm tendon, analytical values obtained using K_s=0 are nearly equal to experimental ones as mentioned before.

Comparing the moment-rotation curves of the grouted and ungrouted specimens with 50 kg/cm^2 initial prestress shown in Figs. 12 and 13, it is noticed that the analyses using the special element model with E/δ=25000 kg/cm^3 are able to estimate the behavior of tested specimens. In the case of the specimens with 35 kg/cm^2 initial prestress, the analytical results using the same element again show similar curves to the experimental results. From these results, the corner element with E/δ=25000 kg/cm^3 may be expected to give reasonable estimation of the rotation at the jointed corner regardless of the values of the initial prestress and bonded condition. However, this conclusion came from the limited data and obiously more experiments is necessary. Meanwhile, in this research the model with E/δ=25000 kg/cm^3 is applied to the rigid framed structure as mentioned in the next chapter.

5. LOAD DEFLECTION HYSTERESIS CURVE IN PRESTRESSED CONCRETE RIGID FRAME

The proposed analysis is applied to the rigid framed specimen tested by Koike et al [4], which is a 1/4-scale model of the pier of Arakawa-Higashi Elevated Bridge, composed of precast concrete members connected by grouted prestressing steels. The specimen is subjected to a lateral cyclic load, and the analyzed

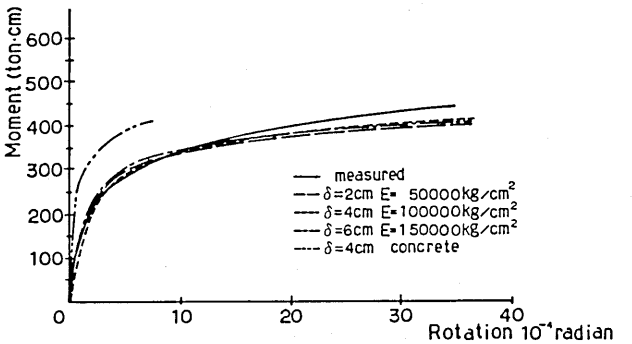

Fig. 12 Measured and calculated rotations at unbonded specimen with 50 kg/cm^2 prestress

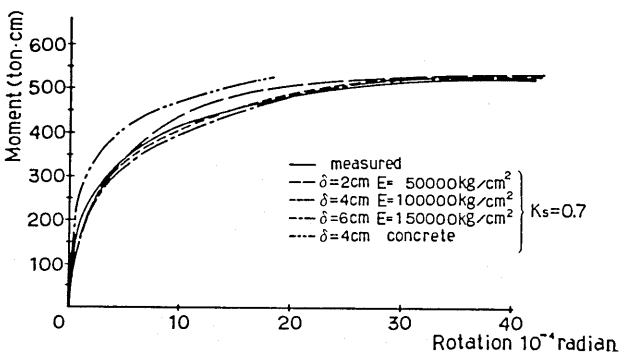

Fig. 13 Measured and calculated rotations at grouted specimen with 50 kg/cm^2 prestress

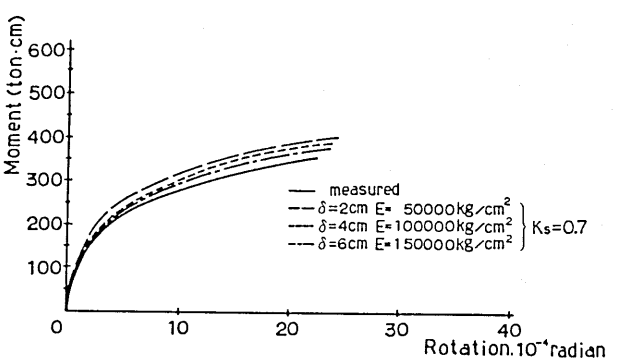

Fig. 14 Measured and calculated rotations at grouted specimen with 35 kg/cm^2 prestress

behavior of the specimen under cyclic loading is compared with the tested data.

Figure 15 indicates the dimension of rigid framed specimen. Firstly the upper beam with box section is prestressed until the stress in concrete is 10 kg/cm^2, and then 10 kg/cm^2 prestress is applied to the column with a box section in order to connect the beam and the column. In this test, the mortar joint is used for the connection between them. The diameter of tendon is 10 mm (yield point is 110 kg/mm^2, and tensile strength is 125 kg/mm^2), and compressive strength of concrete is 400 kg/cm^2.

The discretization as shown in Fig. 16 are used for analysis, and the corner element with δ=2 cm and E=50000 kg/cm^2 are used at the jointed corner shown in the shaded area. Figure 17 shows the measured and calculated load-deflection

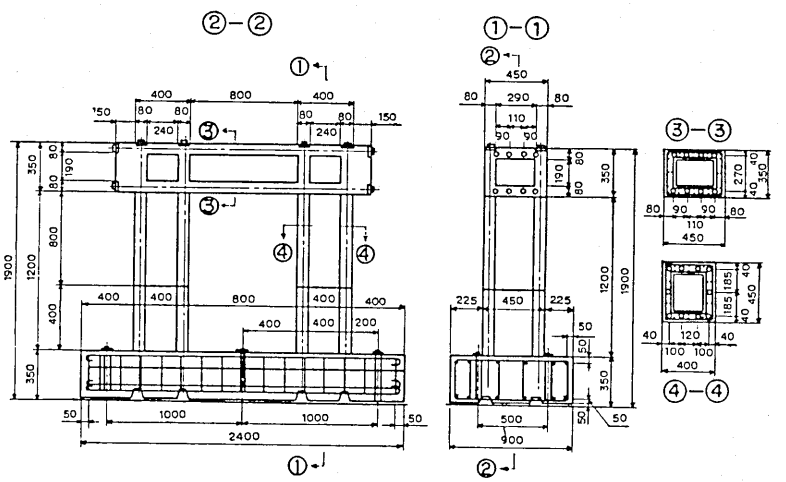

Fig. 15 The rigid framed specimen

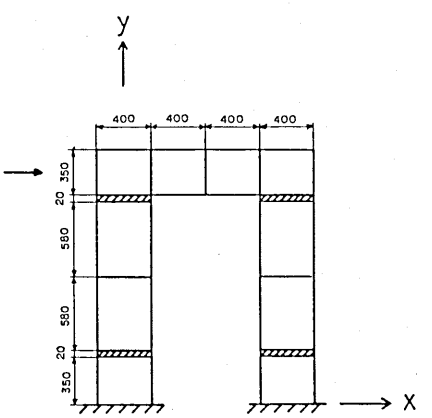

Fig. 16 Discretization of the rigid framed specimen

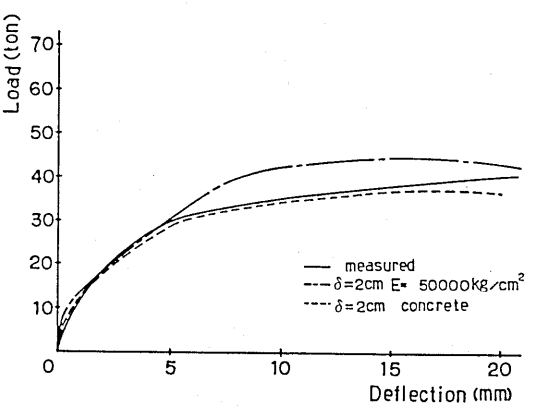

Fig. 17 Load-deflection curves under monotonic loading

curves under monotonic lateral loading. Measured load-deflection curve indicates that the specimen failed at 41 ton after that the deflection increased rapidly at around 30 ton. Calculated load-deflection curve most closely fitted to the measured one is obtained when the sliding coefficient K_s is equal to 0.3. As mentioned before, the perfect bonded condition between concrete and tendon seems not to be assured, as the diameter of tendon increases. In the case of the diameter equal to 22 mm, K_s=0.7 was appropriate for the grouted structure, while in the case of the diameter equal to 7.4 mm, K_s=0.0 was used. Hence, K_s=0.3 may be reasonable because the diameter, 10 mm, in this test is between 7.4 mm and 22 mm. The calaulated load-deflection curve of the specimen without the corner element at the jointed corner is also shown in Fig. 17 with K_s=0.3. Comparing three curves, it may be said that the effect of rotation at the jointed corner becomes remarkable at the deflection around 5 mm by the experiment and the behavior of this kind of rigid framed structure is well simulated by the proposed method with corner elements.

Figure 18 shows the measured and calculated load-deflection hysteresis curves under lateral cyclic load (the maximum load is 10 ton). Although the behavior of the specimen under this load is almost elastic, the residual displacement appears because of the rotation at the jointed corner. Calculated load-deflection curve using K_s=0.3 and the corner element with δ=2 cm and E=50000 kg/cm^2 at the jointed corner shows the good agreement to measured one, although a reversed S shape curve is stressed more clearly than measured one. From these comparisons, the proposed analysis using the corner element at jointed corner can be said to estimate the hysteretic behavior of the rigid framed structure under lateral cyclic loading.

To examine the effect of bond condition on the ultimate strength and deformation characteristics of the frame, the numerical investigation is made. Three cases in the partially bonded condition (K_s=0.0, 0.3, 1.0) are chosen as shown in Fig. 19. It is also recognized that the maximum load decreases from 70 ton to 33 ton according to the condition of the bondage. The load-deflection hysteresis curves (maximum deflection is 5 mm) in these three specimens are compared. Figure 20 shows the results and it is clear that the load-deflection curve in the perfectly unbonded specimen shows pronounced reversed S shape curve and the area surrounded by the loop is very small, which means the capacity of enrgy absorption is very small compared with the bonded specimen.

Those analitically obtained hysteretic character will render substantial help to analyze the seismic behavior of the structure composed by precast concrete members and connected by prestressing.

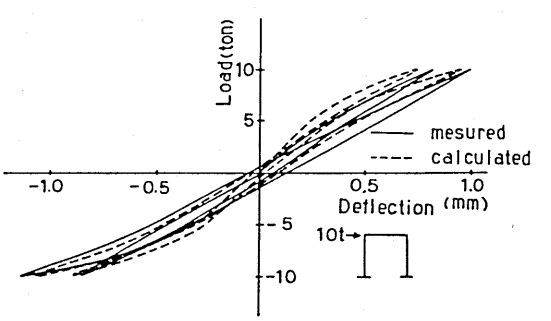

Fig. 18 Load-deflection curves under reversed loading (10 ton)

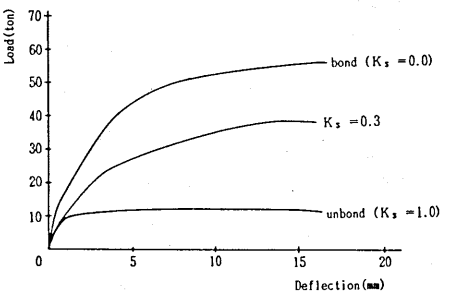

Fig. 19 Effect of the bond condition on the ultimate strength of a frame

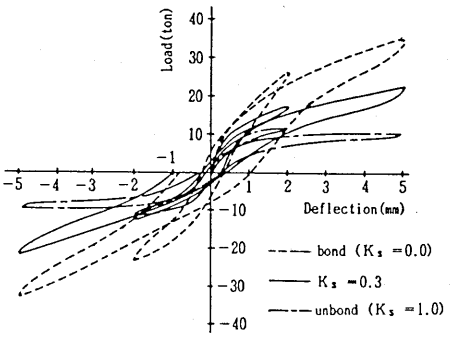

Fig. 20 Effect of the bond condition on the hysteretic behavior of a frame

6. CONCLUSION

From the foregoing study, the following conclusions are obtained.
(1) The proposed method using the finite element analysis can reasonably estimate the hysteretic behavior of the prestressed concrete structures in any bonded condition under cyclic loading considering non-linear stress-strain relation of concrete and steel.
(2) The comparison of the analysis and the test data shows that the grouting of cement milk around prestressing steel do not assure the full bondage between steel and concrete. Often they are in the condition of partial bondage. Therefore, the behavior of a precast concrete rigid frame where its beam columns are connected by prestressing steel should be analysed considering the condition of the bondage.
(3) The rotation at the jointed corner cannot be ignored to estimate the behavior of the rigid framed structure under lateral cyclic loading. The corner element with $E/\delta = 25000$ kg/cm^3 seems to be well for estimating the behavior of the rigid frame. However, the research on developing the corner element may be necessary for applying the method to wider range of prestressed concrete structures with such a rigid corner.

REFERENCES

[1] Tanabe,T. and Hong,P.W., "Unbonded precast elements and its skeletal assemblage", Proc. of JSCE, No. 303, November, 1980
[2] Okada,K. et al, "Studies on fundamental properties of unbonded prestressed concrete beam", Proc. of Prestressed Concrete, Vol. 24, No. 3, May, 1982
[3] Tanabe,T., "Fundamental study on the use of precast concrete members in concrete composite structure", Proc. of JSCE, No. 206, Octorber, 1972
[4] Koike,S. et al, "Design and construction of Arakawa Higashi viaduct in Sobu Line", Journal of JSCE, Vol. 6, No. 6, June, 1968